JOURNAL OF MATERIALS SCIENCE **38** (2003) 2655–2660

Preparation of nm-sized $BaTiO_3$ particles using a new 2-step thermal decomposition of barium titanyl oxalate

S. WADA, M. NARAHARA, T. HOSHINA, H. KAKEMOTO, T. TSURUMI
Department of Metallurgy and Ceramics Science, Graduate School of Science and Engineering, Tokyo Institute of Technology, 2-12-1 Ookayama, Meguro-ku, Tokyo 152-8552, Japan
E-mail: swada@ceram.titech.ac.jp

To obtain inpurity-free and nm-sized barium titanate ($BaTiO_3$) particles, a new 2-step thermal decomposition method from barium titanyl oxalates ($BaTiO(C_2O_4)_2 \cdot 4H_2O$) was proposed. At the 1st step, $BaTiO(C_2O_4)_2 \cdot 4H_2O$ was annealed at 400°C for 1 h in the O_2 flow. The annealing temperature of 400°C was chosen for the following reasons; (1) no formation of $BaCO_3$ and TiO_2 and (2) the complete removal of H_2O and other carbon species. This compound obtained at 400°C was amorphous phase, and its chemical composition was $BaCO_3$-TiO_2. When this compound was annealed in air at higher temperatures, the large $BaTiO_3$ particles were prepared with by-products such as $BaCO_3$. Thus, at the 2nd step, to prevent the crystal growth and the formation of $BaCO_3$, this compound was annealed above 600°C in vacuum. Finally, the $BaTiO_3$ single crystals with a size with 16.5 nm were prepared around 620°C. These $BaTiO_3$ fine particles were characterized using various methods to investigate defects and impurities in the particles. As a result, it was confirmed that there was no impurity in the $BaTiO_3$ lattices. *© 2003 Kluwer Academic Publishers*

1. Introduction

Ferroelectric $BaTiO_3$ fine particles have been used as raw materials for electronic devices such as multilayered ceramic capacitors (MLCC). Recently, with the miniaturization of electronic devices, the down-sizing of MLCC has been developed and accelerated. As a result, the thickness of dielectric layers in MLCC became less than 1 μm, and in the future, it is expected that this thickness will become less than 0.5 μm. Consequently, $BaTiO_3$ raw materials with particle size from a few hundred nm to a few ten nm will be required. However, in ferroelectric fine particles, it was well-known that ferroelectricity decreases with decreasing particle and grain sizes, and disappears below certain critical sizes; this is called the "size effect" in ferroelectrics [1–9]. Therefore, the size effect in ferroelectrics such as $BaTiO_3$ is one of the most important phenomena for the industry and science. To date, some researchers have estimated the critical size to be around 10–20 nm in $BaTiO_3$ fine particles [9–12]. However, this critical size is just an estimated value, and there is no experimental evidence on the critical size. Thus, it is very important to prepare $BaTiO_3$ ferroelectric crystals with sizes below the estimated critical size, and investigate their size effect. However, it is very difficult to prepare impurity-free and nm-sized $BaTiO_3$ crystallites using the conventional wet processes such as the sol-gel [13], hydrothermal [14] and low temperature direct synthesis (LTDS) methods [15, 16]. Especially, the existence of the lattice hydroxyl (OH^-) group was so negative for the ferroelectricity of $BaTiO_3$. This means that the lattice OH^- group was a common problem for the wet-process derived $BaTiO_3$ fine particles [13–16]. Therefore, to prepare impurity-free and nm-sized $BaTiO_3$ crystals below 10 nm, a new innovative preparation method, except for all of the solution methods, is required.

Normally, a thermal decomposition of $BaTiO(C_2O_4)_2 \cdot 4H_2O$ leads to a formation of large $BaTiO_3$ particles over 1 μm, via the intermediate compounds such as $BaCO_3$ and TiO_2 [17–19]. However, there is a significant advantage that a Ba/Ti atomic ratio of the prepared $BaTiO_3$ is completely 1.000 because of the Ba/Ti atomic ratio of 1.000 in $BaTiO(C_2O_4)_2 \cdot 4H_2O$. If nm-sized $BaTiO_3$ particles are prepared from $BaTiO(C_2O_4)_2 \cdot 4H_2O$, it is possible to obtain the impurity-free, defect-free and nm-sized $BaTiO_3$ particles. The large particle sizes of $BaTiO_3$ particles derived from $BaTiO(C_2O_4)_2 \cdot 4H_2O$ is caused by the formation of $BaTiO_3$ via a reaction between $BaCO_3$ and TiO_2 at higher temperatures over 850°C. Thus, it is very important to prevent the formation of these intermediate compounds. For this purpose, the optimum condition for the thermal decomposition of $BaTiO(C_2O_4)_2 \cdot 4H_2O$ must be refined to obtain impurity-free and nm-sized $BaTiO_3$ crystallites, i.e., atmosphere, heating and cooling rate, temperature and soaking time.

In this study, we try to prepare impurity-free and nm-sized $BaTiO_3$ crystallites from $BaTiO(C_2O_4)_2 \cdot 4H_2O$.

0022–2461

For this objective, we propose a new thermal decomposition method of $BaTiO(C_2O_4)_2 \cdot 4H_2O$ using the both atmosphere of the O_2 flow and vacuum.

2. Experimental

2.1. Preparation procedure

Barium titanyl oxalates ($BaTiO(C_2O_4)_2 \cdot 4H_2O$) were prepared at Fuji Titanium Co., Ltd [20]. The Ba/Ti atomic ratio of this compound was 1.000 and the amount of the impurity was less than 0.02% [20]. Fig. 1 shows TGA-DTA curves of this $BaTiO(C_2O_4)_2 \cdot 4H_2O$ measured at a heating rate of 10°C/min in air. Over 710°C, no weight loss was observed, which suggests the formation of $BaTiO_3$ particles. Normally, to prepare $BaTiO_3$ particles from $BaTiO(C_2O_4)_2 \cdot 4H_2O$, the higher temperatures over 1000°C were used in air, but in this case, the larger $BaTiO_3$ particles with sizes around 1 μm were obtained. Hence, if the temperature can decrease down to 710°C, the formation of the smaller $BaTiO_3$ particles with sizes below 100 nm is expected. Thus, the conditions of the normal thermal decomposition in air were optimized using (1) the various temperatures from 100°C to 1000°C and (2) the various soaking times from 0 h to 5 h. On the other hand, to investigate the effect of the atmosphere, the vacuum and the O_2 flow atmosphere were used. This is because (a) a decrease of the decomposition temperature of $BaCO_3$ in vacuum and (b) an easy removal of the carbon species from $BaTiO(C_2O_4)_2 \cdot 4H_2O$ can be expected. In this study, the special designed quartz reactor chamber was used for the ease change from the O_2 flow to the vacuum.

2.2. Characterization

The crystal structure of the products was investigated at 25°C using a powder X-ray diffractometer (XRD) (RINT2000, Rigaku, Cu-ka, 50 kV, 30 mA) and a laser Raman scattering spectrometer (Raman) (NRS-2100, Jusco, 514 nm, 100 mW). The average particle sizes and crystallite sizes were estimated using a transmission electron microscope (TEM) (CM300, Philips, 300 kV) and XRD. The impurity in the products was analyzed using a Fourier transform infrared spectrometer (FT-IR) (SYSTEM 2000 FT-IR, Perkin Elmer) and by differential thermal analysis with thermogravimetry (TGA-DTA) (TG-DTA2000, Mac Science).

3. Results and discussion

3.1. The conventional thermal decomposition method in air

Normally, the thermal decomposition of $BaTiO(C_2O_4)_2 \cdot 4H_2O$ over 1000°C leads to the formation of the large $BaTiO_3$ particles over 1 μm [17–19]. Recently, Kajita and Nishido reported that the thermal decomposition at 850°C leads to the formation of the $BaTiO_3$ particles with sizes of 150 nm [20]. This means that if the conditions for the conventional thermal decomposition are optimized, it is expected to prepare the smaller $BaTiO_3$ particles below 100 nm. Fig. 2 shows a XRD pattern of the products prepared at 700°C for 1 h. As a main product, the formation of the cubic $BaTiO_3$ particles was confirmed while as a by-product, a slight amount of $BaCO_3$ was also observed. The crystallite size D_{111} was calculated from a FWHM of (111) plane around 39° using Scherrer's equation. It should be noted that a $SrTiO_3$ crystal as an external standard for the correction of FWHM. As a result, D_{111} was estimated at around 50 nm. Moreover, TEM observation also revealed that two kinds of particles were observed, and the average $BaTiO_3$ particle size was around 45 nm. On the other hand, when the temperatures below 700°C was used for the thermal decomposition, no $BaTiO_3$ particles were prepared. These results revealed that it was very difficult to prepare the nm-sized $BaTiO_3$ crystallites using the conventional thermal decomposition method in air.

3.2. The thermal decomposition method in vacuum

In vacuum, it can be possible to prepare the impurity-free and nm-sized $BaTiO_3$ fine particles below 50 nm. This is because it is expected that the vacuum atmosphere can make the decomposition temperature of $BaCO_3$ lower than that in air. Thus, the thermal decomposition of $BaTiO(C_2O_4)_2 \cdot 4H_2O$ in vacuum was performed at various temperatures from 500°C to 750°C

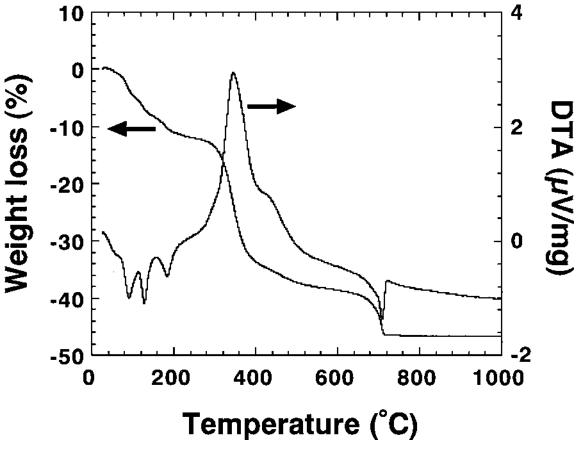

Figure 1 TGA-DTA curves of $BaTiO(C_2O_4)_2 \cdot 4H_2O$.

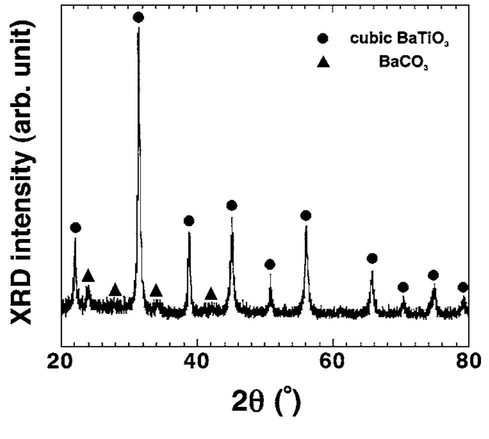

Figure 2 A XRD pattern of the products prepared at 700°C for 1 h in air.

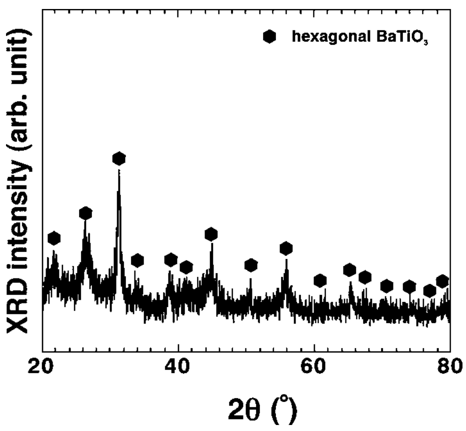

Figure 3 A XRD pattern of the products prepared at 620°C for 1 h in vacuum.

for 1 h. Fig. 3 shows an XRD pattern of the products prepared at 620°C for 1 h in vacuum of 2.3×10^{-2} torr. The FWHMs of all peaks were broadened, which suggests that their crystallite size was extremely small below 10 nm. However, all of the XRD peaks in Fig. 3 were assigned to the hexagonal $BaTiO_3$. Moreover, the color of these particles was completely black. This means that in the hexagonal $BaTiO_3$ particles, there may be the residual carbon or a reduction of titanium ions from +4 to +3, i.e., the hexagonal $BaTiO_3$ was prepared under the reduced atmosphere. Some researchers reported that the reduced atmosphere caused the formation of the hexagonal $BaTiO_3$ because of the oxygen deficiency [21–23]. For our objective, the hexagonal $BaTiO_3$ is an undesirable phase, and the oxygen deficiency leads to the defect structure such as oxygen vacancies in the $BaTiO_3$ lattice. Thus, to remove the residual carbon and oxygen vacancies, these hexagonal $BaTiO_3$ particles were annealed at 400°C for 15 h in the O_2 flow. This oxidizable treatment made the color of the particles gray, which means that the residual carbon still remained, and its XRD pattern was completely the same as Fig. 3. These results revealed that it was very difficult to prepare the impurity-free $BaTiO_3$ crystallites using the thermal decomposition method in vacuum.

3.3. A proposal of a new 2-step thermal decomposition method

The above two methods had several merits and demerits. The thermal decomposition in air could produce the cubic $BaTiO_3$ crystallites, but its problems were the larger crystallite sizes and the formation of $BaCO_3$. On the other hand, the thermal decomposition process in vacuum can produce the nm-sized $BaTiO_3$ crystallites, but its problems are the formation of hexagonal phase and residual carbon. Therefore, if we can combine these two processes, it may be possible to prepare impurity-free and nm-sized $BaTiO_3$ crystallites.

In the former process, the $BaTiO_3$ particles were prepared via intermediates such as $BaCO_3$ and TiO_2. Thus, the reaction of $BaCO_3$ with TiO_2 was the rate-determining stage in the $BaTiO_3$ formation, and its reaction temperature was over 700°C. At the high temperature around 700°C, as the growth rate of $BaTiO_3$ is very fast, the larger $BaTiO_3$ crystallites can be obtained easily. Therefore, to reduce the temperature of the $BaTiO_3$ formation, it is important to prevent the formation of $BaCO_3$ phase as the intermediate.

In the latter process, the nm-sized $BaTiO_3$ particles were prepared as the hexagonal phase with residual carbon. As the above mentioned, this hexagonal phase with the residual carbon was attributed to the reduced atmosphere, which originated from the low temperature decomposition of $BaTiO(C_2O_4)_2 \cdot 4H_2O$ in vacuum. Thus, if the decomposition of $BaTiO(C_2O_4)_2 \cdot 4H_2O$ into an amorphous intermediate with a chemical composition of $BaCO_3$-TiO_2 is performed in the O_2 flow, we can expect that there is no oxygen deficiency in the amorphous intermediates. After this stage, even if the $BaTiO_3$ formation from the amorphous intermediates is done in vacuum, there is no reduced atmosphere. Moreover, it is expected that the vacuum can make the decomposition temperature of $BaCO_3$ much lower. Therefore, to prepare the impurity-free and nm-sized $BaTiO_3$ crystallites from $BaTiO(C_2O_4)_2 \cdot 4H_2O$, it is important to combine two processes, i.e., (I) the low temperature decomposition of $BaTiO(C_2O_4)_2 \cdot 4H_2O$ in the O_2 flow and (II) the $BaTiO_3$ formation from the amorphous intermediates with a chemical composition of $BaCO_3$-TiO_2 in vacuum. We named this new method a 2-step thermal decomposition method.

3.4. The preparation of $BaTiO_3$ crystallites using the 2-step thermal decomposition method

At the 1st step, $BaTiO(C_2O_4)_2 \cdot 4H_2O$ was annealed at various temperatures from 100°C to 450°C for 1 h in the O_2 flow. As a result, below 400°C, it was confirmed that there was no complete decomposition of $BaTiO(C_2O_4)_2 \cdot 4H_2O$, while above 400°C, a slight formation of $BaCO_3$ phase was also detected. It should be noted that the color of the products annealed at 400°C was clear white. This means that a thermal decomposition under the oxygen atmosphere was done without the reduction of titanium ions from +4 to +3. Figs 4 and 5 show an XRD pattern and a Raman scattering spectrum of the products annealed at 400°C for 1 h in the O_2 flow, respectively. In Fig. 4, although

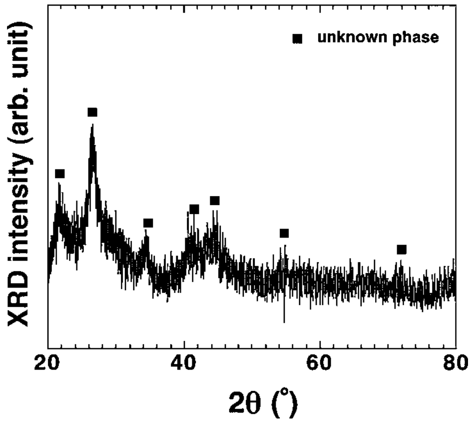

Figure 4 A XRD pattern of the products prepared at 400°C for 1 h in the O_2 flow.

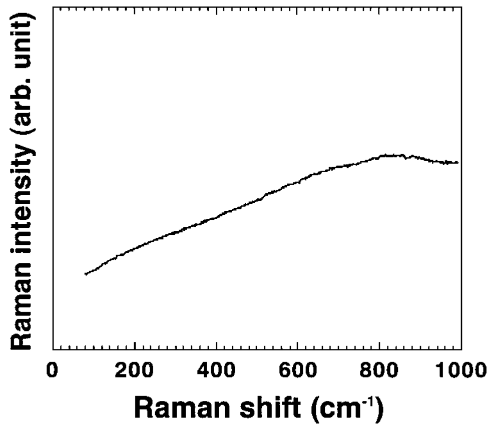

Figure 5 A Raman scattering spectrum of the products prepared at 400°C for 1 h in the O_2 flow.

several unknown broad peaks were observed, most of the products were assigned to the amorphous phase. If $BaTiO(C_2O_4)_2 \cdot 4H_2O$ is completely decomposed into $BaCO_3$ and TiO_2 phases, the weight loss can be calculated at 38.3%. The experimental weight loss at 400°C was almost similar to this one. Therefore, this result suggests that the prepared amorphous phase in Fig. 4 can have the chemical composition of $BaCO_3$-TiO_2. The Raman spectrum in Fig. 5 indicated one significant broad peak. Though this peak was composed of the overlapping of the several broad peaks, we cannot separate the peak into the several peaks. However, this means that there was the disordered lattice vibration like a molecule, i.e., no long range ordering or less long range ordering. Now, we believe that the local structure of the amorphous compounds is closed to the structure with a random network of the $BaCO_3$ and the TiO_2 molecules.

At the 2nd step, the amorphous intermediate compounds were annealed at various temperatures from 550°C to 750°C for 0.5 h in vacuum. As a result, above 600°C, the $BaTiO_3$ formation was confirmed. It should be also noted that the color of these products were clear white. Figs 6 and 7 show an XRD pattern and a Raman scattering spectrum of the products annealed at 620°C for 0.5 h in vacuum, respectively. In Fig. 6, most of the clear peaks were assigned to the cubic $BaTiO_3$ phase. This assignment to the cubic phase was caused by the following two reasons, i.e., (1) no splitting of (002) and (200) planes around 45°, and (2) a good agreement of *a-axis* calculated using (111) plane with *a-axis* calculated using (200) plane. However, two very weak and broad peaks were observed around 27° and 42.4°, and these peaks were assigned to the hexagonal $BaTiO_3$ phase. Moreover, the Raman spectrum in Fig. 7 indicated that most of the peaks were assigned to the tetragonal $BaTiO_3$ phase while a peak at 640 cm^{-1} was assigned to the hexagonal $BaTiO_3$ phase [24, 25]. However, there are some questions about the formation of hexagonal $BaTiO_3$ phase. Recently, Cho *et al.* reported that the cubic $BaTiO_3$ fine crystallites with nanotwins of (111) plane were assigned to the hexagonal phase using XRD and Raman [26–28]. To clear the assignment of these peaks, much investigations will be required. Therefore, now we stop discussing about the formation of the hexagonal $BaTiO_3$ phase or the formation of the nanotwin structure.

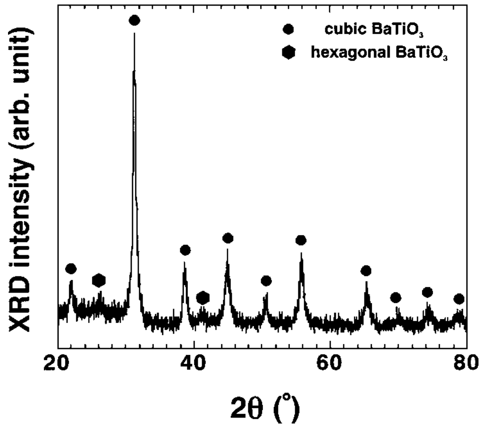

Figure 6 A XRD pattern of the products prepared at 620°C for 0.5 h in vacuum.

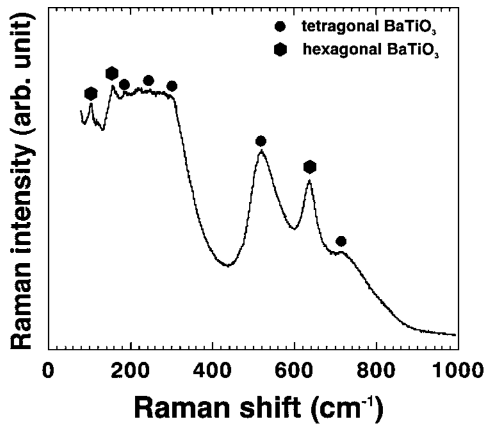

Figure 7 A Raman scattering spectrum of the products prepared at 620°C for 0.5 h in vacuum.

3.5. The characterization of the prepared $BaTiO_3$ crystallites

The $BaTiO_3$ powders annealed at 620°C for 0.5 h in vacuum were characterized using various methods. At first, their crystallite size was estimated by a XRD measurement with a slow scanning rate of 0.1°/min. Fig. 8 shows the (111) plane of the $BaTiO_3$ powders and the (111) plane of the $SrTiO_3$ single crystals as a standard material. The crystallite size D_{111} of the $BaTiO_3$ powders was calculated from a FWHM of (111) plane using Scherrer's equation. It should be noted that a position of peak top and FWHM of (111) plane were corrected using the (111) plane of the $SrTiO_3$ single crystals. As a result, D_{111} was estimated at around 17 nm. Moreover, TEM observation revealed that the average $BaTiO_3$ particle size is around 16.5 nm as shown in Fig. 9a. Fig. 9a also indicates that one particle was a single crystal, and there is no twinning structure. Moreover, its selected area electron diffraction (SAED) pattern (Fig. 9b) revealed that its crystal structure was assigned to the cubic phase of the $BaTiO_3$. These results suggested that the 2-step thermal decomposition method is very effective to prepare the nm-sized $BaTiO_3$ crystallites.

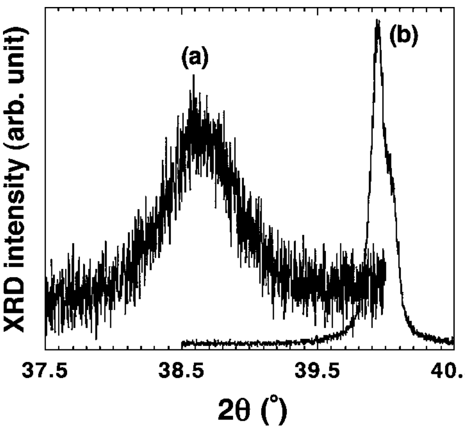

Figure 8 (111) planes of both: (a) the $BaTiO_3$ powders prepared at 620°C for 0.5 h in vacuum and (b) a $SrTiO_3$ single crystal as a reference.

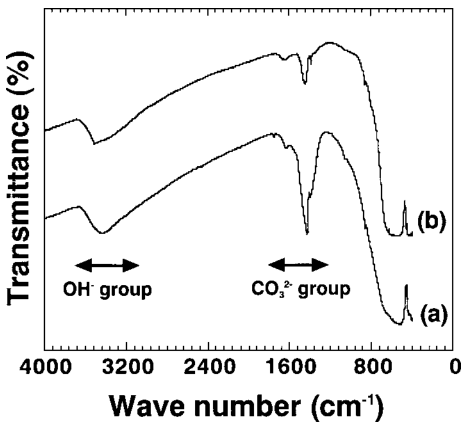

Figure 11 FT-IR spectra of (a) the $BaTiO_3$ powders prepared at 620°C for 0.5 h in vacuum and (b) BT-01 as a reference.

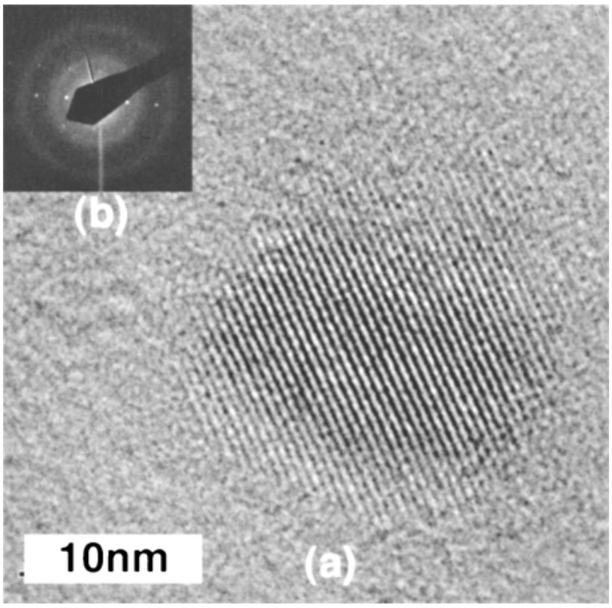

Figure 9 A TEM: (a) bright-field image and (b) SAED pattern of the $BaTiO_3$ powders prepared at 620°C for 0.5 h in vacuum.

To investigate the impurity in the nm-sized $BaTiO_3$ crystallites, TGA-DTA and FT-IR measurements were performed. Fig. 10 shows the TGA-DTA curves of the nm-sized $BaTiO_3$ crystallites annealed at 620°C for 0.5 h in vacuum. This measurement was stopped at 600°C to avoid the crystal growth of the nm-sized $BaTiO_3$ crystallites. A large weight loss of around 4% was detected for the nm-sized $BaTiO_3$ crystallites. In general, it is well-known that the nm-sized particles shows a lot of weight loss over 10% by the adsorbed species because of their huge specific surface areas over 100–200 m^2/g. To confirm the possibility of the weight loss by the adsorbed species, after the 1st measurement of TGA-DTA curves, these powders were cooled in the atmosphere, and the TGA-DTA curves were re-measured using the same powders. As a result, almost same weight loss of around 4% was observed, which suggested that this weight loss was originated from a desorption of the adsorbed species. Moreover, to investigate a kinds of the surface adsorbed species, FT-IR spectra were measured. Fig. 11 shows the FT-IR spectra of the nm-sized $BaTiO_3$ crystallites and BT-01 (hydrothermal $BaTiO_3$ crystallites with a size of 100 nm prepared by Sakai Chemical Industry Co.) as a reference. In Fig. 11, there are only two kinds of species such as OH^- group and $CO_3{}^{2-}$ group in the both powders. The height of these absorption bands in the nm-sized $BaTiO_3$ crystallites was much larger than those in BT-01. This means that the amount of the surface adsorbed species in the nm-sized $BaTiO_3$ crystallites is much larger than that in the BT-01.

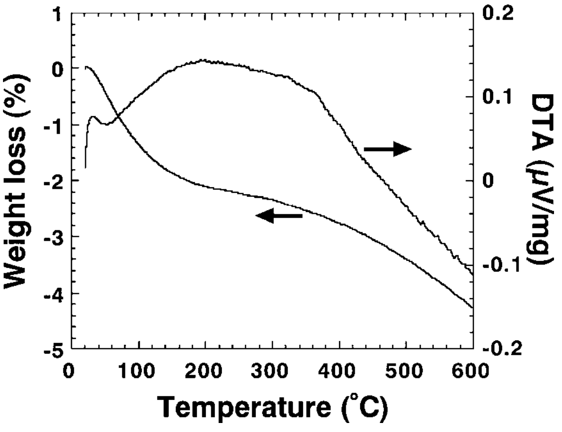

Figure 10 TGA-DTA curves in the $BaTiO_3$ powders prepared at 620°C for 0.5 h in vacuum.

In general, it is well-known that in the hydrothermal $BaTiO_3$ crystallites, there are two kinds of OH^- groups such as (a) a surface adsorbed OH^- group and (b) a lattice OH^- group. The FT-IR measurement is very useful to reveal the existence of these two kinds of OH^- group. Kapphan and Weber reported that proton of the lattice OH^- group can exist in five sites around lattice oxygen in $BaTiO_3$ lattice, and their sharp absorption bands for stretching vibration appear in the narrow range from 3462.5 to 3509.5 cm^{-1} [29]. Fig. 12 indicates FT-IR spectra of the OH^- groups in the nm-sized $BaTiO_3$ crystallites and BT-01. In the BT-01, two kinds of the OH^- group bands were clearly observed, i.e., (I) a sharp band around 3510 cm^{-1} and (II) a broad band from 3000 to 3700 cm^{-1}. On the basis of the report by Kapphan and Weber, the sharp band around 3510 cm^{-1} in BT-01 of Fig. 12 can be assigned to O–H stretching vibration of lattice OH^- group, which suggests that in BT-01, there can exist lattice

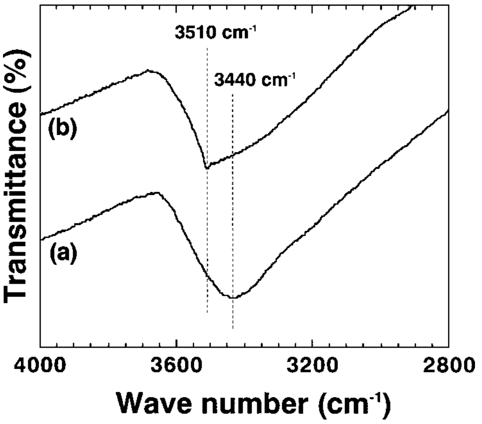

Figure 12 The absorption bands related to the OH$^-$ groups of (a) the BaTiO$_3$ powders prepared at 620°C for 0.5 h in vacuum and (b) BT-01 as a reference.

OH$^-$ group. On the other hand, in the nm-sized BaTiO$_3$ crystallites, there was no sharp band around 3510 cm^{-1} while there was a large broad band from 3000 to 3700 cm^{-1}. These results suggested that there was no lattice OH$^-$ group in the nm-sized BaTiO$_3$ crystallites.

The above characterization revealed that the nm-sized BaTiO$_3$ crystallites prepared by the 2-step thermal decomposition method using BaTiO(C$_2$O$_4$)$_2$ · 4H$_2$O had no impurity in their lattice except for the surface. Thus, we believe that the 2-step thermal decomposition method is very powerful to prepare nm-sized and impurity-free BaTiO$_3$ crystallites. In the future, the dielectric constants of these BaTiO$_3$ crystallites should be measured. For this purpose, much harder work will be required.

4. Conclusion

In this study, the new 2-step thermal decomposition method using BaTiO(C$_2$O$_4$)$_2$ · 4H$_2$O was proposed to obtain inpurity-free and nm-sized BaTiO$_3$ particles. At the 1st step, BaTiO(C$_2$O$_4$)$_2$ · 4H$_2$O was annealed at 400°C for 1 h in the O$_2$ flow. This compound obtained at 400°C was amorphous phase with the chemical composition of BaCO$_3$-TiO$_2$. At the 2nd step, the amorphous compound was annealed under vacuum above 600°C. Finally, BaTiO$_3$ single crystals with a size of 16.5 nm were prepared around 620°C. Their characterization was also done using various methods, and especially, the impurity in these nm-sized BaTiO$_3$ crystallites was investigated. As a result, as the impurities, the surface adsorbed OH$^-$ and CO$_3{}^{2-}$ groups and the were detected, but no lattice OH$^-$ group was detected using IR. This suggests that the nm-sized BaTiO$_3$ crystallites have no impurity in their lattice. Therefore, the 2-step thermal decomposition method using BaTiO(C$_2$O$_4$)$_2$ · 4H$_2$O was very effective to prepare the nm-sized and inpurity-free BaTiO$_3$ crystallites. This means that the 1st step for a study of the size effect was achieved. At the next step, using the 2-step thermal decomposition method, the BaTiO$_3$ particles with various particle sizes will be prepared, and their size dependence of the structure and some physical properties will be investigated.

Acknowledgments

The authors would like to thank Mr. M. Nishido of Fuji Titanium Co., Ltd. for preparing high purity barium titanyl oxalates. This study was partially supported by (1) Research Development Program of University-Industry Alliance—A Matching Funds Approach from JSPS), (2) a Grant-in-Aid for Scientific Research (**12450267**) from the Ministry of Education, Science, Sports and Culture, Japan, and (3) Takayanagi Foundation for Electronics, Science and Technology.

References

1. K. KINOSHITA and A. YAMAJI, *J. Appl. Phys.* **45** (1976) 371.
2. G. ARLT, D. HENNINGS and G. DE WITH, *ibid.* **58** (1985) 1619.
3. K. ISHIKAWA, K. YOSHIKAWA and N. OKADA, *Phys. Rev.* B **37** (1988) 5852.
4. K. UCHINO, E. SADANAGA and T. HIROSE, *J. Amer. Ceram. Soc.* **72** (1989) 1555.
5. H. IKAWA, in "Dielectric Ceramics; Ceramic Transactions," Vol. 32 (Amer. Ceram. Soc., 1993) p. 19.
6. M. H. FREY and D. A. PAYNE, *Phys. Rev.* B **54** (1996) 3158.
7. S. WADA, T. SUZUKI and T. NOMA, *J. Ceram. Soc. Jpn.* **104** (1996) 383.
8. K. ISHIKAWA, T. NOMURA, N. OKADA and K. TAKADA, *Jpn. J. Appl. Phys.* **35** (1996) 5196.
9. D. McCAULEY, R. E. NEWNHAM and C. A. RANDALL, *J. Amer. Ceram. Soc.* **81** (1998) 979.
10. M. TANAKA and Y. MAKINO, *Ferroelectric Lett.* **24** (1998) 13.
11. M. R. SRINIVASAN, M. S. MULTANI, P. AYYUB and R. VUAYARAGHAVAN, *Ferroelectrics* **51** (1983) 137.
12. A. J. BELL, A. J. MOULSON and L. E. CROSS, *ibid.* **54** (1984) 147.
13. H. MATSUDA, M. KUWABARA, K. YAMADA, H. SHIMOOKA and S. TAKAHASHI, *J. Amer. Ceram. Soc.* **81** (1998) 3010.
14. S. WADA, T. SUZUKI and T. NOMA, *J. Ceram. Soc. Jpn.* **103** (1995) 1220.
15. S. WADA, H. CHIKAMORI, T. NOMA and T. SUZUKI, *J. Mater. Sci.* **35** (2000) 4857.
16. S. WADA, H. CHIKAMORI, T. NOMA, T. SUZUKI and T. TSURUMI, *J. Ceram. Soc. Jpn.* **108** (2000) 728.
17. K. IIZUMI, K. SOBATA and K. KUDAKA, *ibid.* **92** (1984) 4.
18. T. ISSHIKI, K. NISHIDO, M. SHIOJIRI, H. NOGUCHI, Y. DEGUCHI and H. YAMAMOTO, *Elect. Techno.* **31** (1998) 202.
19. J. XU, S. TSUTAI, S. HAYASHI, M. SUGI and Z. NAKAGAWA, *J. Ceram. Soc. Jpn.* **107** (1999) 27.
20. T. KAJITA and M. NISHIDO, Ext. Abst. the 9th US-Japan Seminar Dielect. Piezoelect. Ceram., Okinawa (1999) p. 425.
21. R. M. GLAISTER and H. F. KAY, *Proc. Phys. Soc.* **76** (1960) 763.
22. M. WAKAMATSU, N. TAKEUCHI, G.-C. LAI and S. ISHIDA, *J. Ceram. Soc. Jpn.* **95** (1987) 1181.
23. N. TAKEUCHI, H. TANAKA, M. WAKAMATSU, Y. SAKABE and K. WAKINO, *ibid.* **98** (1990) 836.
24. N. G. EROR, T. M. LOEHR and B. C. CORNILSEN, *Ferroelectrics* **28** (1980) 321.
25. Y. AKISHIGE, K. KAMISHIMA, J. NAKAHARA and E. SAWAGUCHI, *ibid.* **152** (1994) 225.
26. W.-S. CHO, E. HAMADA and K. TAKAYANAGI, *J. Appl. Phys.* **81** (1997) 3000.
27. W.-S. CHO, *J. Phys. Chem. Solids* **59** (1998) 659.
28. E. HAMADA, W.-S. CHO and K. TAKAYANAGI, *Phil. Mag.* A **77** (1998) 1301.
29. S. KAPPHAN and G. WEBER, *Ferroelectrics* **37** (1981) 673.

Received 29 July 2002
and accepted 9 April 2003